JOURNAL OF MATERIALS SCIENCE **38** (2003) 3501–3508

Transverse fatigue crack propagation behavior in equine cortical bone

D. R. SHELTON
Division of Materials Science and Engineering, College of Engineering, University of California, Davis, CA 95616, USA

R. B. MARTIN
Orthopaedic Research Laboratory, School of Medicine, University of California, Davis, CA 95616, USA

S. M. STOVER
J. D. Wheat Veterinary Orthopedic Research Laboratory, School of Veterinary Medicine, University of California, Davis, CA 95616, USA

J. C. GIBELING*,†
Division of Materials Science and Engineering, College of Engineering, University of California, Davis, CA 95616, USA
E-mail: jcgibeling@ucdavis.edu

Stress fractures stem from the initiation and propagation of fatigue cracks through bone, and fatigue damage may play a role in many other orthopaedic problems, such as hip fractures in the elderly. The objective of this investigation was to measure fatigue crack propagation rates in cortical bone. Specific aims were to determine fatigue crack growth rate, da/dN, as a function of alternating stress intensity factor, ΔK, for equine third metacarpal cortical bone tissue; to determine whether the resulting data followed the Paris law; and to test the hypothesis that crack growth rates differ between dorsal and lateral regions. Compact type specimens oriented for transverse crack growth were subjected to fatigue under Mode I loading. The da/dN vs. ΔK data for the dorsal specimens revealed a Paris law exponent of 10.4 ($R^2 = 0.82$), comparable to that for ceramics. These data also exhibited an apparent threshold stress intensity factor of 2.0 MPa $\cdot$ m$^{1/2}$. It was not possible to obtain similar results for lateral specimens because all cracks deviated from the desired transverse path and ran longitudinally in spite of the use of side grooves to constrain the crack path. However, the results for lateral specimens were not due to a failure of the test method, but reflect dramatic differences in fatigue crack propagation resistance between the two cortical regions. These results are consistent with clinical observations that stress fractures in the third metacarpus typically occur in the mid-diaphysis of the dorsal cortex, but not in the lateral cortex.

1. Introduction

Stress fractures stem from the initiation and propagation of fatigue cracks through bone [1], and fatigue damage may play a role in many other orthopaedic problems, such as hip fractures in the elderly [2]. It has become increasingly clear that fatigue resistance is an extremely important property of bone [3], and one may postulate that biological processes conferring fatigue resistance arose early in vertebrate evolution. In addition, bone has the ability to repair itself by the process of remodeling, in which damaged material is replaced by freshly formed bone. Although remodeling is thought to be an important component of fatigue resistance [4, 5], understanding the mechanical resistance of bone tissue itself to damage is equally important.

A number of investigators have adopted the view that cortical bone is mechanically analogous to fiber reinforced ceramic matrix composites [6, 7]. Briefly, the structure of equine and human cortical bone is characterized by osteons consisting of a central nutrient-carrying Haversian canal surrounded by circular layers of collagen and hydroxyapatite. These osteons can be thought of as short, hollow fibers (approximately 200 μm diameter by 4 mm long) embedded in a mineralized, brittle, matrix with cement lines forming the interface between these two constituents. These 'fibers'

* Author to whom all correspondence should be addressed.
† *Present address*: Department of Chemical Engineering and Materials Science, University of California, One Shields Ave., Davis, CA 95616, USA.

may improve mechanical properties in a specific direction, the same way fibers toughen brittle ceramics. They also can deflect cracks and increase the energy absorbed through interfacial debonding. When cracks propagate transverse to the longitudinal axis of a bone, pull-out of the osteon fibers can be observed [6, 8].

Numerous studies have shown that microstructure and mechanical properties may vary regionally within individual bones. Riggs *et al*. [9] found the cranial cortex of the equine radius to be stiffer in both tension and compression than the caudal cortex. They noted that cranial specimens had more longitudinally oriented collagen fibers, were denser and were significantly less remodeled than specimens taken from the caudal cortex. The lateral region of the equine third metacarpal bone was found to be monotonically stronger and stiffer than the dorsal region [10–12], but dorsal specimens had longer fatigue lives [11].

The *in vitro* fatigue life of bone has been investigated using unnotched specimens [11, 13–15], but these studies have provided no direct information about the growth of fatigue cracks. To learn more about this phenomenon, one must study crack growth in a prenotched specimen under cyclically applied loads. The customary form of the relationship between fatigue crack growth rate (da/dN) and alternating stress intensity factor (ΔK) exhibits three characteristic regions (Fig. 1). At low ΔK, the crack growth rates asymptotically decrease toward a threshold, ΔK_{th}. and at high ΔK, K_{max} approaches the fracture toughness of the material, K_c. The Paris law regime at intermediate ΔK is described by a power law relation of the form:

$$da/dN = A(\Delta K)^m \quad (1)$$

where A is a constant and m typically has values of 2 to 4 for metals and alloys, 7 to 20 for ceramics and 10 to 20 for fiber reinforced ceramic matrix composites [16, 17].

Published data for fatigue crack growth rates in cortical bone are limited to the studies of Vashishth *et al*. [18] and Wright and Hayes [19]. Both groups presented da/dN vs. ΔK results for longitudinal crack growth (in the direction of the long axis of the osteon "fibers") in bovine cortical bone. For rates between about 2×10^{-6} and 8×10^{-5} m/cycle, Vashishth *et al*. reported an m value of 1.73 for specimens cycled between 10 and 40 N. For their second group of specimens, cycled between 10 and 80 N, the reported value of m was 5.54, and, in this case crack growth rates varied between about 8×10^{-5} and 2.5×10^{-4} m/cycle. Similarly, for crack growth rates between 7.2×10^{-7} and 3.4×10^{-4} m/cycle, Wright and Hayes reported m values from 2.8 to 5.1, depending on test frequency and bone (femur or tibia). However, neither of these studies differentiated between cortical regions within a bone. More recently, Taylor [20] has developed a theoretical da/dN vs. ΔK curve for microcracks in cortical bone based on stiffness changes during cyclic loading.

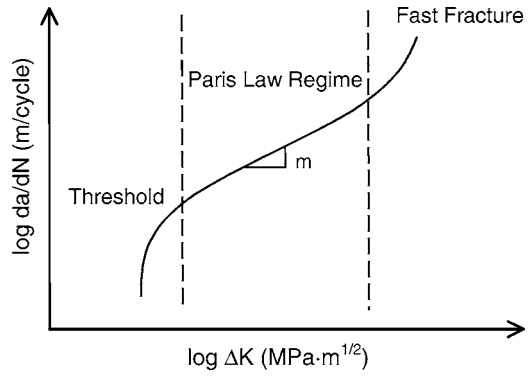

Figure 1 Schematic illustration of fatigue crack propagation results (da/dN vs. ΔK) for an engineering material showing three characteristic regions of behavior.

The fracture resistance of cortical bone is extremely anisotropic, with K_c significantly lower for longitudinal cracking than for transverse cracking [8]. However, some transverse crack growth must occur, at least initially, in diaphyseal fractures [8]. Nevertheless, da/dN vs. ΔK curves have not been measured for transverse crack growth, nor have regional variations in such crack growth rates been explored. Therefore, we sought to measure fatigue crack growth for transverse crack propagation in the lateral and dorsal cortices of equine third metacarpal bone, and to determine if the Paris law could describe the results. Because other mechanical properties of this bone vary by cortical region, we hypothesized that fatigue crack growth rates would vary regionally as well.

2. Materials and methods

Five pairs of equine third metacarpal (cannon) bones were obtained from five Thoroughbred racehorses (mean age 5.2 years, range 4–7 years) after necropsy for problems unrelated to the cannon bone. None of these bones exhibited visual evidence of acute periosteal bone deposition. Individual bones were wrapped in paper towels moistened with saline, and stored frozen at −20°C before machining and afterwards until testing.

Sections were taken from the middle of the diaphysis immediately proximal and distal to the midline and each proximal or distal section was assigned to provide either a lateral or dorsal specimen so that one of each was obtained from each leg (Fig. 2) for a total of 20 specimens. No property variations were expected over the short distance along the diaphysis from which the specimens were obtained [21]. Location (proximal or distal), region (dorsal or lateral) and leg (left or right) were distributed as evenly as possible within and among the 5 horses.

Specimens were machined in accord with ASTM standard E647 [22] except that the included notch angle was 60 degrees, the notch height was 1.80 mm, and 45 degree V-shaped side grooves were added to constrain cracks to propagate transversely [23] (Fig. 3). Machining was performed at room temperature under copious irrigation with water-soluble oil. Specimens were oriented such that the longitudinal axis of the bone was parallel to the loading direction (Fig. 3, double-headed arrows).

Specimens were tested in an MTS 810 servohydraulic materials testing system. Because the small

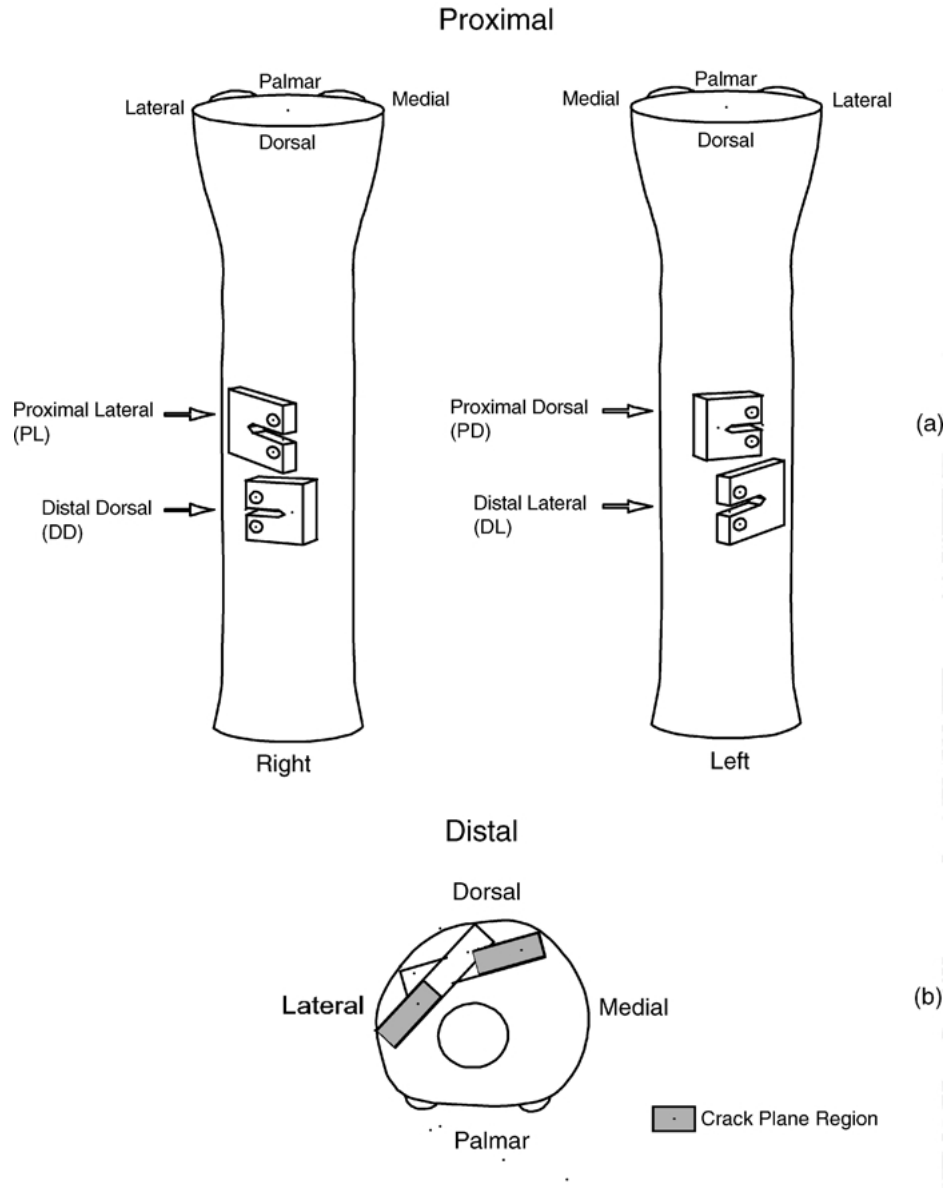

Figure 2 Illustration of the locations of the four specimens taken from a pair of equine third metacarpal bones (a). In two of the 5 horses, the leg (left vs. right) was reversed. Cortical location of dorsal and lateral $C(T)$ specimens in transverse section (b) [25].

specimen size precluded the use of a standard crack opening displacement (COD) gage, COD was measured with an MTS model 632.26 E-30 extensometer attached to the front face of the specimen with elastic bands. Loads were monitored with an Interface model 1010AF 2224 N (500 lb.) load cell. Previous work on fracture of bone has shown this to be a reliable method to determine specimen compliance [24, 25]. Specimens were mounted in stainless steel clevis grips similar to those described in ASTM E399-90 [26]. A drip system was used to keep specimens wet and warm (at $37 \pm 2^{\circ}$C) during testing with calcium buffered normal (0.9% NaCl) saline [27] containing Bath Clear Microbicide (Fisher Scientific, Pittsburgh, PA) added (1 mL/L) to prevent enzymatic degradation. The testing system was controlled by a personal computer running MTS 790.40 Fatigue Crack Growth (FCG) software version 4.2 A.

All tests were conducted at a loading frequency of 2 Hz and a load ratio, $R(=K_{\min}/K_{\max})$, of 0.1. Crack length was measured by monitoring the change in specimen compliance as the fatigue crack grew [16, 22]. Specimen compliance, C, defined as the slope of the COD vs. load curve, was calculated from a least squares fit of the data. During crack growth, compliance is related to crack length through a fifth order polynomial [28]:

$$\frac{a}{W} = 1.000 - 4.500U_{\mathrm{x}} + 13.157U_{\mathrm{x}}^2 - 172.551U_{\mathrm{x}}^3 + 879.944U_{\mathrm{x}}^4 - 1514.671U_{\mathrm{x}}^5 \quad (2)$$

based on

$$U_{\mathrm{x}} = \frac{1}{1 + \sqrt{B_{\mathrm{eff}}EC}} \quad (3)$$

where $B_{\mathrm{eff}} = \sqrt{BB_{\mathrm{n}}}$ is the effective specimen thickness [29] and E is the effective elastic modulus for each specimen determined from a preliminary loading ramp using the compliance calibration and the known,

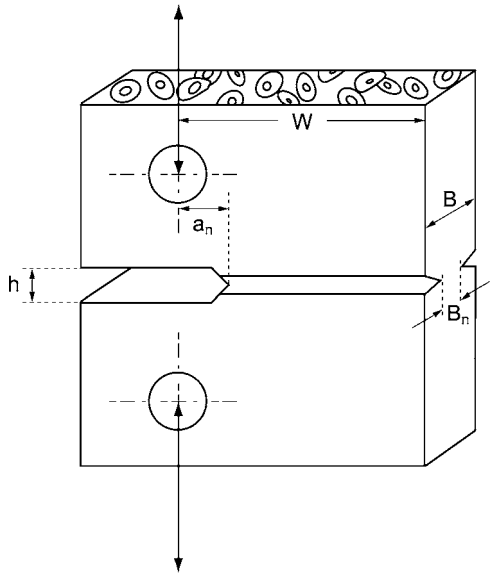

Figure 3 Illustration of a compact type, $C(T)$, specimen oriented for transverse crack growth ($W = 20.32$ mm, $B = 5.0$ mm, $B_n = 3.0$ mm and $a/W = 0.5$ initially).

machined notch length. Data were monitored continuously and saved at crack length increments of 0.05 mm. Final fatigue crack lengths were measured optically from the fracture surfaces of the dorsal specimens and were found to be within ±5% of the final crack length as calculated using the compliance method. This finding further validates the use of the extensometer to measure COD rather than the more common crack opening displacement gage.

Specimens were randomly assigned to the test matrix shown in Table I where initial ΔK values ranged between 1.5 to 3.6 MPa · m$^{1/2}$ for the lateral specimens and between 2.03 and 4.0 MPa · m$^{1/2}$ for the dorsal specimens. This selection of different initial ΔK was necessary because the total amount of crack growth was limited by the specimen width. This limitation precluded the possibility of a single specimen being tested over the entire range of da/dN of interest. Two slightly different procedures were used to generate sharp fatigue precracks 11.96 mm in length in accordance with ASTM E647 §8.3.1 [22]. For specimens that were designated to be fatigue tested at an initial $\Delta K < 3.6$ MPa · m$^{1/2}$, the precrack was produced by cyclic tensile loading at constant R and declining ΔK as suggested in the applicable standard [22]. In these cases, the initial precracking ΔK was 1.4 times the intended initial ΔK of the subsequent fatigue test, and ΔK declined during precracking to a value equal to the initial ΔK for the fatigue crack growth test. For fatigue tests that were to be run at higher ΔK values, it was thought that the large initial load imposed by this procedure could cause specimens to fail prematurely. Therefore, specimens that were to be fatigue tested at $\Delta K \geq 3.6$ MPa · m$^{1/2}$ were precracked using a constant ΔK equal to the initial ΔK value used during the subsequent fatigue crack growth test.

The fatigue crack growth tests were conducted under ΔK control with ΔK varying during the test by gradual, uniform steps calculated according to the expression:

$$\Delta K_n = \Delta K_o \exp[C'(a_n - a_o)]. \quad (4)$$

Here, ΔK_n is the value corresponding to the current crack length, a_n, ΔK_o, is the value corresponding to the last measured crack length, a_o, and C' is the normalized K gradient. ΔK was calculated using the polynomial expression given in ASTM E647 §9.3.1, modified for the grooved compact type specimen [8, 23], i.e.,

$$\Delta K = \frac{\Delta P}{\sqrt{BB_n}\sqrt{W}} \frac{2 + \left(\frac{a}{W}\right)}{\left[1 - \left(\frac{a}{W}\right)\right]^{3/2}} \left[0.886 + 4.64\left(\frac{a}{W}\right) - 13.32\left(\frac{a}{W}\right)^2 + 14.72\left(\frac{a}{W}\right)^3 - 5.60\left(\frac{a}{W}\right)^4\right] \quad (5)$$

where ΔP is the load range. All but two specimens were fatigue tested with a normalized K gradient (C') of −0.08/mm (ΔK decreasing tests). The remaining two specimens were used to map the upper region of the da/dN vs. ΔK curve and were tested with ΔK increasing ($C' = +0.08$/mm). These values were based on the recommendation of Saxena *et al.* [30] as well as ASTM guidelines for fatigue testing [22]. Tests were terminated when the crack lengths reached 0.9 W or the specimen fractured.

After testing, each dorsal specimen was soaked for one hour in 100% ethanol containing 1% basic fuchsin stain to mark the position of the crack front. Each of these specimens was returned individually to the load

TABLE I Fatigue testing matrix[a]

	Initial value of ΔK (MPa · m$^{1/2}$)						
Specimen location	1.50[b]	2.025[b]	2.25[b]	2.50[b]	3.15[b]	3.60[c]	4.00[c]
Dorsal		*1163 LDD* *1581 LDD*		1580 RPD	1166 RDD *1579 LPD*	1580 LDD	1166 LPD
Lateral	1580 LPL	1163 LPL	1580 RDL 1581 LPL		1163 RDL	1166 RPL	

[a]The first four numbers identify the horse. The first letter following the horse number corresponds to the side (L = left, R = right), the next letter refers to the location (P = proximal, D = distal), and the last letter refers to the cortical region (D = dorsal, L = lateral). For example, 1163 LDD describes a specimen that came from the distal dorsal cortex of the left leg of horse number 1163. Specimens in italics fatigue tested under ΔK increasing conditions, all others under ΔK decreasing conditions.
[b]Precracked by the decreasing ΔK method.
[c]Precracked by the constant ΔK method.

frame and fractured by loading at a constant rate. The (transverse) fracture surfaces were removed by making a cut across the specimen, approximately 2 mm below the fracture surface using an Isomet 2000 (Buehler, Ltd., Lake Bluff, IL) diamond blade cut-off saw. The cut pieces were then glued to a metal stub and sputter coated with approximately 300 angstroms of gold for observation via scanning electron microscopy (SEM) at 25 kV (ISI Model DS-130, International Scientific Instruments, Inc., Pleasanton, CA).

3. Results

The relationship of crack growth rates to associated alternating stress intensity factors for transverse crack propagation in dorsal specimens (Fig. 4) is similar in form to that expected for an engineering material as illustrated schematically in Fig. 1. As indicated in Table I, these results represent data from a total of 7 specimens including some from left and right legs and both proximal and distal locations. The remaining 3 dorsal specimens were lost during setup or testing. At low ΔK, the data approach an apparent threshold stress intensity value of 2.0 MPa $\cdot$ m$^{1/2}$ (Fig. 4). At high ΔK, the data asymptotically approach the condition for which $K_{\max}$ corresponds to the fracture toughness of 4.38 MPa $\cdot$ m$^{1/2}$ for [24] this material. At intermediate values of ΔK, between crack growth rates of 10^{-5} to 10^{-8} m/cycle, the data are described by the Paris law (Equation 1) with m equal to 10.4 ($R^2 = 0.82$).

It was not possible to obtain a da/dN vs. ΔK plot for lateral specimens because, in spite of the side grooves and after an immeasurably small amount of crack propagation in the transverse direction, all cracks deviated from the desired path and ran longitudinally, parallel to the fiber-like osteons (Fig. 5). These results represent a total of 6 specimens from both right and left legs and the proximal and distal locations (Table I). The remaining 4 specimens were lost during setup or testing. The results obtained for the lateral specimens do not reflect a failure of the test method, but demonstrate the dramatic differences in transverse fatigue crack propagation resistance between the two cortical regions.

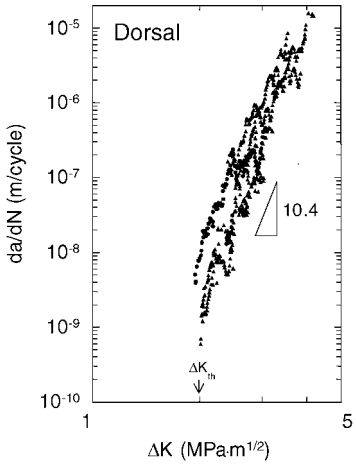

Figure 4 Fatigue crack growth data for equine third metacarpal bone, dorsal cortex. Circles and triangles represent data for specimens taken from right and left legs respectively.

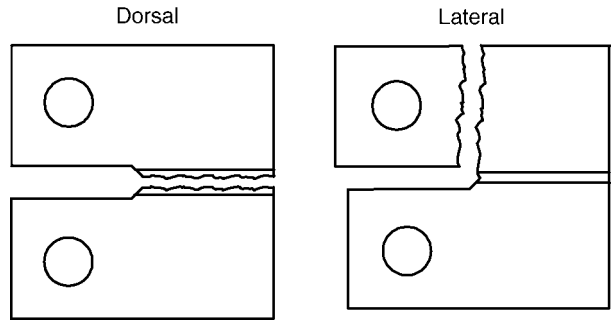

Figure 5 Schematic illustration of fracture profiles in dorsal and lateral specimens. Cracks propagated transversely in the dorsal specimens but always turned and ran longitudinally in the lateral specimens.

Areas of the fracture surfaces of dorsal specimens corresponding to fatigue crack growth were rough and uneven due to osteon pullout (Fig. 6a). A relatively high density of osteons was observed in specimens from this region, suggesting that the bone had undergone significant remodeling. The final monotonic specimen fracture after staining could be identified by an abrupt change from the rough appearance of the fatigue crack growth region to the relatively flat, smooth surface associated with rapid crack propagation. The vertical fracture surfaces of the lateral specimens exhibited delamination along lamellar interfaces within and between osteons in the bone tissue (Fig. 6b).

4. Discussion

The Paris law exponent values ranging from 2.8 to 5.1 as reported by Wright and Hayes [19] and between 1.73 and 5.54 as reported by Vashishth *et al.* [18] are significantly lower than the value of 10.4 obtained in this study. One reason for this difference may be that both of these research groups grew cracks longitudinally in their cortical bone specimens whereas the cracks were grown transversely in this study. In addition, microstructural variations between the horse and cow bone used in these two studies are unknown. However, bovine cortical bone tends to be primary plexiform bone that is orthotropic in its elastic properties [31], whereas the equine cannon bone specimens tested in this study, due to the age of the horses, were secondary remodeled bone [32] which is transversely isotropic [7]. The effect of these microstructural variations on fatigue crack growth behavior is unknown.

Despite these microstructural differences, comparison of the results suggests that fatigue crack growth in cortical bone may be less sensitive to variations in the applied stress intensity in the longitudinal direction than in the transverse direction. That is, the large value of m for the transverse data means that a very small change in the applied ΔK leads to a large change in the crack growth rate. Furthermore, the Paris law exponent of 10.4 obtained in this study is within the range expected for a ceramic or ceramic matrix composite to which bone is often compared [7]. In transversely oriented specimens, the crack must pass through osteons that behave like the fibers in a fiber-reinforced composite. These structures serve to increase fatigue resistance since energy that would be available for crack

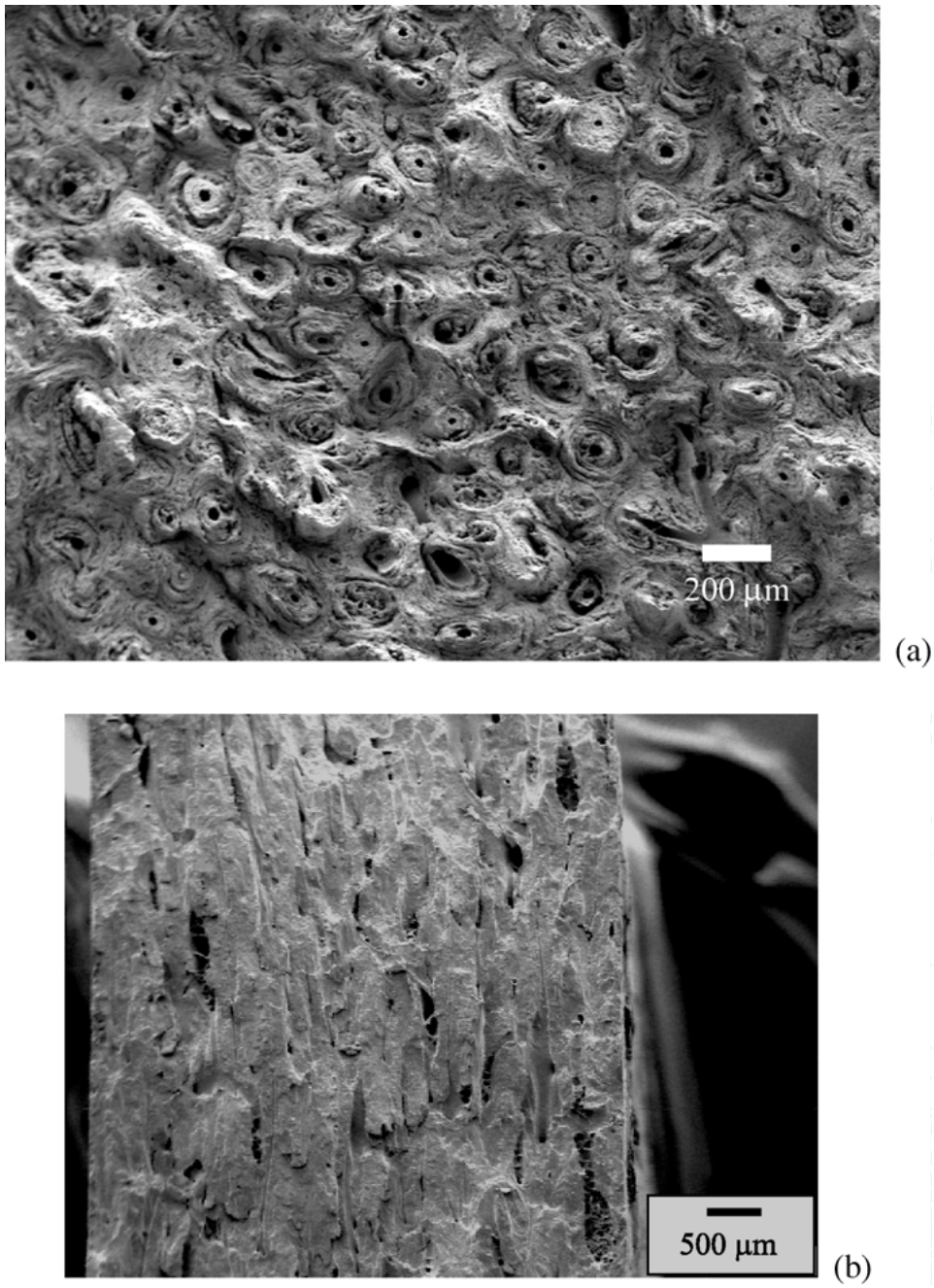

Figure 6 SEM micrograph of (a) the transverse fatigue fracture surface of a dorsal specimen and (b) the vertical fracture surface of a lateral specimen.

propagation is instead utilized to pull out, delaminate and break the osteons. The cement lines (osteon/matrix interfaces) also help to increase fatigue resistance because their poor fiber-matrix bonding and differences in stiffness and energy transfer qualities relative to the bone matrix serve to slow crack growth [33, 34].

Comparison of crack growth rates indicates that for a given ΔK, cracks grow faster in the longitudinal direction in bovine cortical bone than they do in the transverse direction in equine cortical bone. At an applied ΔK of 3.0 MPa $\cdot$ m$^{1/2}$ our results indicate a crack growth rate of about 1×10^{-6} m/cycle for transverse cracks in equine third metacarpal bone whereas the crack growth rate for longitudinal crack growth in bovine femur as reported by Wright and Hayes was approximately twice as high, or 2×10^{-6} m/cycle [19]. Again, this difference is similar to that expected for a ceramic matrix composite tested in different orientations.

Several studies, including this one, have found variations in mechanical and fatigue properties between cortical regions in bone. It is reasonable to assume that the variations in fatigue crack growth rates reported here are due to well-established microstructural differences between cortical regions of equine third metacarpal bones. Of particular interest is the study of Martin *et al.* [35] in which they used circularly polarized light to study collagen fiber orientation in specimens from Thoroughbred equine cannon bones that had been fatigue tested in 3-point bending [11]. These specimens had more "hooped" osteons in lateral regions than dorsal regions, and the majority of secondary osteons in the dorsal cortex had alternating layers of birefringent lamellae. "Hooped" osteons have circumferentially oriented collagen fibers only in the outermost lamellae whereas alternating birefringence patterns indicate collagen fiber orientations that vary between circumferential and

longitudinal throughout the osteonal wall. On average, collagen fibers were more longitudinally oriented in the lateral than in the dorsal cortex, but collagen fiber orientation did not correlate with fatigue life [36]. It was also reported that osteon pullout occurred in the dorsal specimens but never in the lateral specimens [37], consistent with the observations shown in Fig. 6a. Finally, dorsal regions had smaller secondary osteons [35] and greater porosity [38] than lateral regions.

It is likely that regional differences in fatigue crack growth resistance are also manifestations of differences in loading history and its relationship to bone microstructure. The current tests were conducted under cyclic tension, whereas *in vivo*, at a medium speed trot (3.6 m/s), the equine cannon bone is loaded in bending with the neutral axis passing through the dorsal cortex at a slight angle such that only the most periosteal tissue of the dorsal cortex is loaded in tension [39, 40]. During all phases of gait, this portion of the dorsal region is loaded in tension, but a portion of the lateral region is alternately loaded in tension and compression. The observed variations in microstructure between lateral and dorsal cortices appear to result from mechanical adaptation of these regions to this loading scenario. The presence of larger osteons and the abundance of longitudinally oriented collagen fibers in the lateral region may explain why it is highly resistant to transverse crack propagation. This result is consistent with clinical observations that stress fractures in the mid-diaphysis of the third metacarpus typically occur in the dorsal cortex [41]. The fact that these fractures occur at all implies that the bone has adapted poorly to its loading conditions (i.e., if the dorsal region had more longitudinally oriented collagen fibers the occurrence of stress fractures would be reduced). However, as Nunamaker [42] has pointed out, only 5% of a Thoroughbred racehorse's training time is spent at full racing speed, the balance is at lower speeds. Presumably, their bones are adapted to the lower stresses and strains experienced at slower speeds and the higher loading experienced during racing may lead to fatigue damage accumulation and possible fracture.

5. Conclusions

Fatigue crack propagation in cortical bone from the third metacarpal of Thoroughbred racehorses exhibits characteristics similar to ceramic matrix composites when tested for cracking transverse to the axes of the osteons (fibers). Crack propagation rates in the dorsal cortex are characterized by a Paris law exponent of 10.4 and an apparent threshold ΔK_{th} of 2.0 MPa $\cdot$ m$^{1/2}$. We were unable to quantitatively substantiate our hypothesis that crack growth rates would vary between cortical regions. In spite of the use of side grooves on the $C(T)$ specimens, in all cases fatigue cracks in the lateral cortex deviated from the transverse direction and grew longitudinally, parallel to the osteon axes. However, our results clearly demonstrate that the lateral region is more resistant to transverse fatigue crack propagation than the dorsal region in grooved $C(T)$ specimens. This observation is consistent with the fact that *in vivo* stress fractures in the equine third metacarpus occur in the dorsal region and may reflect the influence of mechanical adaptation due to different *in vivo* loading conditions.

Acknowledgments

This research was supported by a NSF Graduate Research Fellowship (DRS) and National Institutes of Health Grant AR41644. We also acknowledge the assistance of the California Horse Racing Board Postmortem Program and the California Animal Health and Food Safety Laboratory System.

References

1. G. L. NORWOOD, *Proc. Amer. Assn. Equine Pract.* **24** (1978) 319.
2. S. M. BOWMAN, X. E. GUO, D. W. CHENG, T. M. KEAVENY, L. J. GIBSON, W. C. HAYES and T. A. MCMAHON, *J. Biomech. Eng.* **120** (1998) 647.
3. D. B. BURR, M. K. FORWOOD, D. P. FYHRIE, R. B. MARTIN, M. S. SCHAFFLER and C. H. TURNER, *J. Bone Mineral Res.* **12** (1997) 6.
4. D. B. BURR, R. B. MARTIN, M. B. SCHAFFLER and E. L. RADIN, *J. Biomech.* **18** (1985) 189.
5. H. M. FROST, in "Osteoporosis," edited by H. F. DeLuca, H. M. Frost, W. S. S. Jee and C. C. Johnston (University Park Press, Baltimore, 1980).
6. K. PIEKARSKI, *J. Appl. Phys.* **41** (1970) 215.
7. R. B. MARTIN, *Mater. Sci. Forum* **293** (1999) 5.
8. J. C. BEHIRI and W. BONFIELD, *J. Biomech.* **22** (1989) 863.
9. C. M. RIGGS, L. C. VAUGHAN, G. P. EVANS, L. E. LANYON and A. BOYDE, *Anat. Embryol.* **187** (1993) 239.
10. G. BIGOT, A. BOUZIDI, C. RUMELHART and W. MARTIN-ROSSET, *Med. Eng. Phys.* **18** (1996) 79.
11. V. A. GIBSON, S. M. STOVER, R. B. MARTIN, J. C. GIBELING, N. H. WILLITS, M. B. GUSTAFSON and L. V. GRIFFIN, *J. Orthop. Res.* **13** (1995) 861.
12. C. M. LES, J. H. KEYAK, S. M. STOVER, K. T. TAYLOR and A. J. KANEPS, *ibid.* **12** (1994) 822.
13. M. B. SCHAFFLER, E. L. RADIN and D. B. BURR, *Bone* **11** (1990) 321.
14. D. R. CARTER, W. E. CALER, D. M. SPENGLER and V. H. FRANKEL, *Acta Orthop. Scand.* **52** (1981) 481.
15. M. B. SCHAFFLER, E. L. RADIN and D. B. BURR, *Bone* **10** (1989) 207.
16. S. SURESH, "Fatigue of Materials," 1st ed. (Cambridge University Press, Cambridge, 1991).
17. T. L. ANDERSON, "Fracture Mechanics: Fundamentals and Applications," 2nd ed. (CRC Press, Boca Raton, FL, 1995).
18. D. VASHISHTH, K. E. TANNER, J. C. BEHIRI and W. BONFIELD, in "Proceedings of the 40th Annual Meeting, Orthopaedic Research Society, New Orleans, Louisiana, February 21–24, 1994" (Orthopaedic Research Society, 1994) p. 429.
19. T. M. WRIGHT and W. C. HAYES, *J. Biomed. Mater. Res.* **7** (1976) 637.
20. D. TAYLOR, *J. Biomech.* **31** (1998) 587.
21. C. M. LES, S. M. STOVER, J. H. KEYAK, K. T. TAYLOR and N. H. WILLITS, *ibid.* **30** (1997) 355.
22. ASTM Standard Test Method for Measurement of Fatigue Crack Growth Rates, Designation: E647-95, in "Annual Book of ASTM Standards" Vol. 3.01 (American Society for Testing and Materials, Philadelphia, 1995) p. 578.
23. T. L. NORMAN, D. VASHISHTH and D. B. BURR, *J. Biomech.* **25** (1992) 1489.
24. C. L. MALIK, S. M. STOVER, R. B. MARTIN and J. C. GIBELING, *ibid.* **36** (2003) 191.
25. C. L. MALIK, J. C. GIBELING, R. B. MARTIN and S. M. STOVER, *ibid.* **35** (2002) 701.

26. ASTM Standard Test Method for Plane Strain Fracture Toughness of Metallic Materials, Designation: E399-90, in "Annual Book of ASTM Standards" Vol. 3.01 (American Society for Testing and Materials, Philadelphia, 1993) p. 412.
27. M. B. GUSTAFSON, R. B. MARTIN, V. A. GIBSON, D. H. STORMS, S. M. STOVER, J. C. GIBELING and L. V. GRIFFIN, *J. Biomech.* **29** (1996) 1191.
28. J. A. KAPP, *J. Test. Eval.* **19** (1991) 45.
29. ASTM Standard Test Method for J_{IC}, a Measure of Fracture Toughness, Designation: E813-89, in "Annual Book of ASTM Standards" Vol. 3.01 (American Society for Testing and Materials, Philadelphia, 1989) p. 732.
30. A. SAXENA, S. J. HUDAK, JR., J. K. DONALD and D. W. SCHMIDT, *J. Test. Eval.* **6** (1978) 167.
31. R. B. MARTIN and J. ISHIDA, *J. Biomech.* **22** (1989) 419.
32. S. M. STOVER, R. R. POOL, R. B. MARTIN and J. P. MORGAN, *J. Anat.* **181** (1992) 455.
33. D. B. BURR, M. B. SCHAFFLER and R. G. FREDERICKSON, *J. Biomech.* **21** (1988) 939.
34. J. D. CURREY, *Quarter. J. Microsc. Sci.* **103** (1962) 111.
35. R. B. MARTIN, V. A. GIBSON, S. M. STOVER, J. C. GIBELING and L. V. GRIFFIN, *Bone* **19** (1996) 165.
36. R. B. MARTIN, S. T. LAU, P. V. MATHEWS, V. A. GIBSON and S. M. STOVER, *J. Biomech.* **29** (1996) 1515.
37. S. M. STOVER, R. B. MARTIN, V. A. GIBSON, J. C. GIBELING and L. V. GRIFFIN, in "Proceedings of the 41st Annual Meeting, Orthopaedic Research Society, Orlando, Florida, February 13–16, 1995" (Orthopaedic Research Society, 1995) p. 129.
38. R. B. MARTIN, S. M. STOVER, V. A. GIBSON, J. C. GIBELING and L. V. GRIFFIN, *J. Orthop. Res.* **14** (1996) 794.
39. T. S. GROSS, K. J. MCLEOD and C. T. RUBIN, *Trans. Annual Mtg. Orthop. Res. Soc.* **16** (1991) 420.
40. *Idem.*, *J. Biomech.* **25** (1992) 1081.
41. D. M. NUNAMAKER, D. M. BUTTERWECK and J. BLACK, *Amer. J. Vet. Res.* **52** (1991) 97.
42. D. M. NUNAMAKER, D. M. BUTTERWECK and M. T. PROVOST, *J. Orthop. Res.* **8** (1990) 604.

Received 8 August 2001
and accepted 8 January 2003